Construction and Building Materials 274 (2021) 121793

Contents lists available at ScienceDirect

Construction and Building Materials

journal homepage: www.elsevier.com/locate/conbuildmat

Iron based shape memory alloys as shear reinforcement for bridge girders

Christoph Czaderski [a,*], Moslem Shahverdi [a], Julien Michels [b]

[a] Empa, Structural Engineering, Dübendorf, Switzerland
[b] re-fer AG, Seewen, Switzerland

HIGHLIGHTS

- Iron-based shape memory alloy in the form of U-shaped ribbed bars.
- Used in combination with sprayed cement based mortar.
- For shear strengthening of reinforced concrete (RC) beams.
- Prestressed shear strengthening.
- Reduction of beam deflections, stresses in internal steel stirrups, crack widths.

ARTICLE INFO

Article history:
Received 17 August 2020
Received in revised form 5 November 2020
Accepted 20 November 2020
Available online 6 December 2020

Keywords:
Shear strengthening
Reinforced concrete
Shape memory alloys
Prestressed strengthening
Digital image correlation
Shear cracks

ABSTRACT

Considerable age of a very high number of bridges conjointly with a steadily increasing amount of traffic and changes in design philosophy (e.g. earthquake engineering) have made maintenance needed and retrofitting become more and more important over the years. Retrofitting can become necessary both for flexure or shear enhancements. Existing steel solutions for shear strengthening are very laborious and complex, and the durability of the steel construction is questionable. As an alternative to steel solutions, carbon fiber reinforced polymer (CFRP) sheets or strips are used for shear strengthening of reinforced concrete beams. But, prestressing of CFRP sheets or strips is hardly applicable. However, a prestressing of a shear strengthening has the advantages that the width of existing shear cracks can be reduced and the stresses in the internal steel stirrups are reduced.

Therefore, in this study, a new iron-based shape memory alloy ('memory-steel') in the form of U-shaped (stirrups) ribbed bars with a nominal diameter of 12 mm were used in combination with sprayed mortar for shear strengthening of reinforced concrete (RC) structures. The memory-steel bars were activated with electric resistive heating. The activation resulted in a prestress of about 300 N/mm^2 in the memory-steel reinforcement and consequently in vertical compressive stresses in the web of the RC beams. Large-scale experiments on T-beams with a height of 0.75 m and a total length of 5.2 m were performed to show the practicability and efficiency of the memory-steel shear strengthening. Promising results have shown that the new strengthening system works well in practice. The shear capacity could be increased significantly. Furthermore, at the serviceability limit state, the prestressed memory-steel stirrups reduced the overall beam deflections, the stresses in the internal steel stirrups, the number of cracks, and the crack widths.

1. Introduction

Built infrastructure, such as buildings, bridges, highways, dams, tunnels, water supply systems, and many others guarantee the proper functioning of our daily living standards. Their structural integrity in combination with their construction and maintenance costs is one of the key challenges civil engineers are confronted with. Since infrastructure (beside buildings) is in its large majority public-owned, investments often directly derive from tax money and hence are of high public interest. For several decades already, reinforced concrete is a very well-known and efficient building material and represents nowadays by far the most spread construction material all over the world. Considerable age of a very

* Corresponding author at: Empa, Empa, Structural Engineering Research Laboratory, Überlandstrasse 129, 8600 Dübendorf, Switzerland.
E-mail address: christoph.czaderski@empa.ch (C. Czaderski).

https://doi.org/10.1016/j.conbuildmat.2020.121793
0950-0618/

high number of for instance bridges conjointly with a steadily increasing amount of traffic and changes in design philosophy (e.g. earthquake engineering) have made maintenance needed and retrofitting become more and more important over the years. Maintenance costs represent nowadays a very important part of all investments related to a specific construction type. In the United States, for instance, maintenance costs for bridges are above 10 billion USD per year according to a study by the American Society of Civil Engineers [1].

Prestressing a reinforced concrete structure is an even more efficient technique in terms of durability and serviceability, as cracks and deformations can be reduced or at least prevented from further growing. This technique is a common construction method all over the world: a large number of bridges are fully or partially designed this way, especially to overcome large spans and to guarantee the mentioned satisfactory behavior under service loads. Prestressed tendons are mainly used in the longitudinal direction (flexural reinforcement). Very rare is the usage of prestressing for shear strengthening because it is very complicated from a practical point of view. However, according to for example the Swisscode SIA 166 "Externally bonded reinforcement" [2], the provision is given that, if a beam with shear cracks at serviceability state shall be strengthened for shear, then, the strengthening shall envelop the total beam height and must be prestressed. The advantages if the shear strengthening is prestressed are [3]: (i) the shear cracks can be reduced or even closed, (ii) the existing internal steel stirrups are partly unloaded what increases their fatigue resistance and (iii) the strengthening takes immediately additional loads. However, prestressing of the shear strengthening is hardly possible today with the conventional systems. Fig. 1 shows a (prestressed) shear strengthening example on a Swiss bridge. It can be seen that such solutions are very laborious and complex, and the durability of the steel construction is questionable. As an alternative to the steel solutions, carbon fiber reinforced polymer (CFRP) sheets or strips are used for shear strengthening of reinforced concrete beams [4–9]. However, prestressing of the CFRP sheets or strips is hardly possible. The only CFRP system, which can prestressed, is the unbonded carbon fiber–reinforced polymer (CFRP) strap system from the company Carbo-Link, a spin-off from Empa in Switzerland, which was originally developed at Empa [3,5,10–12].

However, the application of shape memory alloy stirrups can provide the possibility to implement prestressed shear strengthening. Shape memory alloys have the characteristic that they, after having been pre-deformed, move partly back to their initial shape when subjected to high temperatures. This characteristic leads to a completely new philosophy in terms of a prestressing technique for concrete constructions based on shape memory effects [13–15]. The hydraulic jacks and the mechanical anchorage system of conventional prestressing techniques would become obsolete. Therefore, prestressing is easier and cheaper when using SMA, because ducts, anchor heads, and oil hydraulic jacks are not necessary anymore. The material in the shape of a ribbed bar is initially prestrained and can subsequently be placed into a concrete structure or externally installed and being surrounded afterwards with an additional cementitious layer (e.g. shotcrete or sprayed mortar), [16]. Once the surrounding material has sufficiently cured, heating is applied to the steel bars by resistive heating. Since the bars cannot move back to their initial state as they are blocked by the concrete, they will be prestressed and consequently, the concrete will undergo compression stresses. (Iron-based) shape memory alloys further have the advantage that in case of a future demolition, the material can be fully recycled and hence offers a strong contribution to the circular economy. In Europe and North America, stainless steel production is almost solely based on recycling (melting and re-casting) scrap material. Iron-based shape memory alloys can, due to their metallurgical composition (see description below for the alloy composition of the Fe-SMA used in this study), be treated in a similar manner as stainless steel and hence be re-introduced into the casting process.

Lastly, fire protection is also far less invasive compared to for instance FRP products, which due to the low glass transition temperature of the resin require substantial measures to protect them from high temperatures. The behavior of iron based shape memory alloys under elevated temperatures is comparable to steel [17], which leads to simpler and less cost-intensive protection systems compared to FRP's.

The most commercially available shape memory alloy on the market is Nickel/Titanium (NiTi). However, the commercial application of NiTi is limited due to the high costs of raw materials and processing. The effectiveness of NiTi for prestressing is often restricted by their relatively narrow thermal hysteresis, which is inadequate for the large and stable recovery stresses required for civil engineering applications. In a study presented in [18], a concrete beam was reinforced with NiTi wires. It was found that if the NiTi wires are heated, they are prestressed and have a larger stiffness, however, if they are not heated, they lose the prestress and have a reduced stiffness. As an alternative, iron-based shape memory alloys such as Fe-Mn-Si based alloys are more suitable for this type of application due to their wide transformation hysteresis, lower cost, and high elastic stiffness compared to conventional Nitinol alloys [15,19]. Sato et al. discovered the shape memory effect in these alloys in 1982 [20]. A Fe-Mn-Si based alloy especially feasible for construction was invented at Empa [21]. The composition of the alloy is Fe-17Mn-5Si-10Cr-4Ni-1(V,C) (mass%).

Fig. 1. Example of a conventional shear strengthening on a Bridge near Solothurn in Switzerland.

Related products were then developed in collaboration with re-fer AG founded in 2012 to commercialize these reinforcements [22]. The Fe-Mn-Si based alloy is generally known as 'memory-steel'. memory-steel is produced in the form of ribbed bars and strips [14,23–25].

The research in the field of SMA for shear strengthening started already in 2001 [26]. Strengthened successfully a RC beam in the laboratory and also a real bridge in the US by using iron based shape memory alloy rods. Unfortunately, according to the knowledge of the authors, this research was not continued. Only again in 2016 [27], published a study on pseudoelastic Ni-Ti (commonly known as Nitinol or NiTi) continuous spiral shear reinforcements for rectangular RC beams to obtaining more ductile shear failures. The beams reinforced with the Ni-Ti rectangular spirals showed high ductility in shear, with very high deflections and large crack widths at failure. In the same institute, proof-of-concept researches on concrete beams with the dimensions 80x150x900 mm were performed. Firstly [28], presented an investigation on shear strengthening of the rectangular beams by using 3 mm diameter Ni-Ti-Nb wires externally installed around the beams, forming a pseudo-spiral, to actively confine, or transversally prestress, the RC members. Secondly [29], used 12.5 and 25 mm wide and 0.5 mm thick iron based shape memory alloys (Fe-SMA) strips. The strips were wrapped around the rectangular cross-section, connected with a buckle, and then activated (prestressed) what means that they were heated with a heat gun. The shear strengthened beams showed a significant higher failure load and for the beams strengthened with activated strips, the appearance of shear cracks was delayed, there were fewer shear cracks, and the deflections of beams were significantly lower, which revealed the benefits of this active shear strengthening technology. Lastly [30], recently published a study on the shear strengthening of real-scale RC T-beams by means of U-shaped Fe-SMA strips. The T-beams had a length of 5.5 m and a height of 0.55 m. All the beams failed in shear and the retrofitted beams showed a 30% increased shear strength. The active shear strengthening delayed the appearance of cracks and reduced their crack width at service loads. However, in the study, problems with the mechanical fasteners to fix the Fe-SMA strips to the web occurred so that the proper performance of the Fe-SMA strips were prevented and it was concluded for future research another type of mechanical anchorage or a fully wrapping method shall be used.

[31] used also 25 mm wide and 0.5 mm thick iron-based shape memory alloys (Fe-SMA) strips to shear strengthen 2.3 m long and 0.35 m high T-beams. Although there were some issues with the anchorage of the strips at the flanges and more development work would be necessary, generally, they found a significant increase in both strength and ductility of the strengthened beams compared to the control specimens.

In this research, a large-scale experimental campaign on RC beams, which were strengthened for shear by a new innovative method is presented. The new method uses U-shaped ribbed memory-steel bars, which are embedded in an additional sprayed mortar layer and are prestressed after the mortar has cured.

2. Experiments

Large-scale reinforced concrete (RC) beams with a shear deficient reinforcement were constructed, strengthened for shear by using U-shaped ribbed memory-steel bars embedded in an additional sprayed mortar layer, and lastly loaded to failure. The aim was to show the efficiency of the new memory-steel shear strengthening method. The main focus was on the effect of the prestress of the stirrups. To study the effect of the prestress, reference beams that were not prestressed were examined as comparison and several measurements during the loading up to failure were performed to quantify the effect of the prestressed stirrups. A further aim of the investigation was to show the practicability of the new strengthening technique for on-site applications.

2.1. Strengthening procedure

The strengthening procedure on the RC beams included the following working steps:

1. Drilling of holes in the flange (Fig. 5)
2. Concrete hammering in the strengthening area (Fig. 2)
3. Sandblasting of the hammered zones to remove all loosely concrete parts
4. Installation of the U-shaped ribbed memory-steel stirrups (Fig. 3)
5. Application of formwork for the repair mortar (Fig. 4)
6. Application of a bonding primer (Sika MonoTop-910N) to the concrete surface
7. Application of the repair mortar (Sika MonoTop-412N) by spraying (Fig. 4)
8. Filling of the holes in the flange with cementitious grout (SikaGrout-314)
9. Activation of the memory-steel stirrups by resistive heating

The thickness of the sprayed mortar layer was approximately 30 mm. Therefore, the U-shaped ribbed memory-steel stirrups had a cover of 10–20 mm in the test beams. However, similar as in usual reinforced concrete, the concrete protects the reinforcement for corrosion and larger covers are recommended for real applications.

2.2. Beam geometry and materials

The geometries of the beams were chosen so that they are representative of onsite application; the height, the web width, and the span were 0.75 m, 0.16 m, and 4.3 m, respectively (Fig. 5 and Fig. 7). A further aim of the experiments was to reach shear failure so that the behavior of the new shear strengthening method under shear loading and shear failure could be investigated. Therefore, the moment/shear ratio a/d (a = distance between load and support, d = static height) was chosen as 1800/665 = 2.7, what is a good ratio for shear failure (Fig. 7) according to the "Kani valley", see e.g. [32]. Additionally, a high strength flexural reinforcement (4 bars Ø=30 mm, yield strength of 843 MPa, tensile strength of 945 MPa) was used to avoid premature flexural failure. The internal steel stirrups with a diameter of 8 mm had a yield strength of 504 MPa and tensile strength of 560 MPa. Three stirrups were placed in each shear span. The locations of the stirrups are displayed in Fig. 7.

Fig. 2. Concrete hammering on one of the test beams.

Fig. 3. Installed memory-steel stirrups on one of the test beams. The red bolts are polymer dowels for fixation of the memory-steel stirrups on the concrete surface. (For interpretation of the references to colour in this figure legend, the reader is referred to the web version of this article.)

Fig. 4. Application of spray mortar to one of the test beams. Timber formwork on the sides and the bottom.

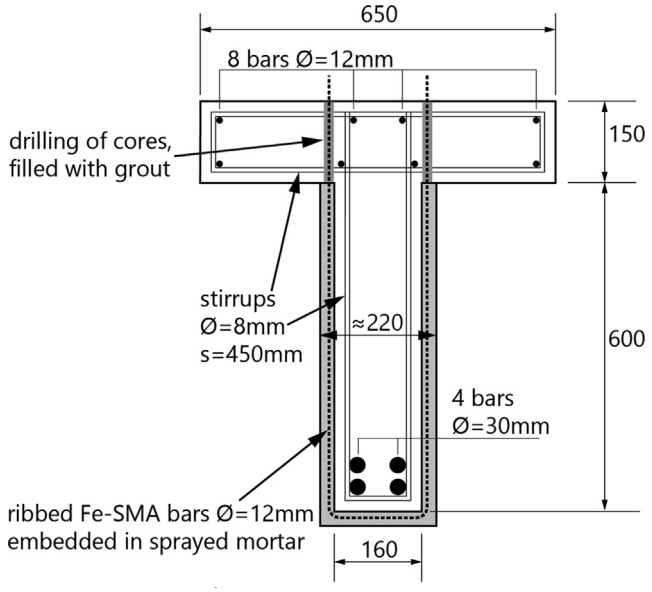

Fig. 5. Cross-section of the test beams including the strengthening method.

The concrete was produced and delivered from a local concrete plant. It had a maximum aggregate size of 16 mm and the obtained strengths are given in Table 1.

The ribbed memory-steel bars with a nominal diameter of 12 mm (effective approximately 11 mm) were delivered by the company re-fer. They were prestrained to 4% and bent afterwards in a U-shape. Tensile mean strength R_m of the bars was 810 N/mm^2

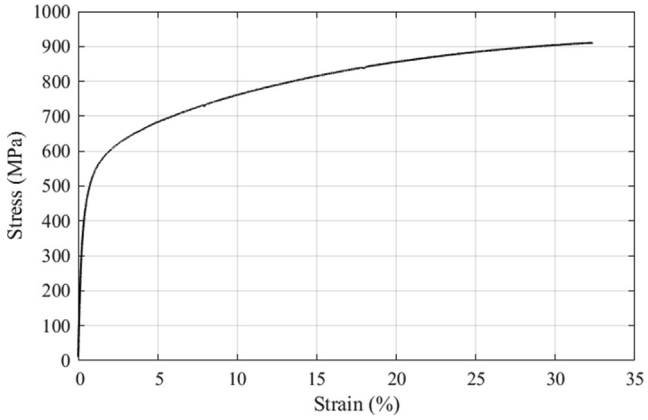

Fig. 6. Stress–strain diagram of a ribbed memory-steel bar, similar as used in this study.

with a mean strain at failure A_{gt} of 20%. A typical stress–strain diagram is displayed in Fig. 6. The first part of it corresponds to Action (1) as discussed below, see Fig. 8.

On the surface of the hammered concrete, the bonding primer Sika MonoTop-910 N was used. According to the technical data sheet of the supplier, it is a cementitious, polymer-modified one-component coating material containing silica fume and has a compressive strength after 28 days of approximately 35 N/mm^2. The repair mortar Sika MonoTop-412 N is, according to the technical data sheet of the supplier, a 1-component, fiber reinforced, low shrinkage repair mortar, and has a compressive and flexural tensile strength after 28 days of approximately 55 and 8 N/mm^2, respectively. For the filling of the holes in the flange, SikaGrout-314 was used. According to the technical data sheet of the supplier, it is a 1-component, cementitious, expanding, low shrinkage grout and has a compressive strength after 28 days of approximately 90 N/mm^2.

2.3. Experimental program

The experimental program is presented in Table 1 and Fig. 7. Beam 1 was the unstrengthened reference beam. Beams 2 and 3 had the same strengthening scheme (i.e. three memory-steel stirrups), however, the memory-steel stirrups were only activated (prestressed) in Beam 2, so that the beneficial effect of prestress could be studied. Beams 5 and 6 were strengthened with five memory-steel stirrups, whereas again only the memory-steel stirrups in Beam 5 were activated.

Furthermore, the reference beam without strengthening (Beam 1) was repaired after the failure test and tested again (Beam 4), [33].

2.4. Prestraining, activation, and loading of memory-steel stirrups

The main actions for the shear strengthening by using memory-steel are illustrated in Fig. 8a): **Action (1):** The memory-steel reinforcements were pre-strained to a strain level of about 4%, afterward fully released and then formed in U-shape. In the next step, they were embedded in the sprayed mortar as described above (Fig. 4). After the mortar had cured, the beams were transported to the laboratory. Then, the memory-steel U-shaped stirrups were activated by resistive heating, **Action (2)** in Fig. 8a) and b). For that reason, the electric power supply from the company re-fer AG, which is specially designed for activation of memory-steel, was connected by cooper clamps (Fig. 9 and Fig. 10). By using a current of 400 A (current density of 3.5 A/mm^2), one stirrup after the other was heated to approximately 160 °C, see the measured tempera-

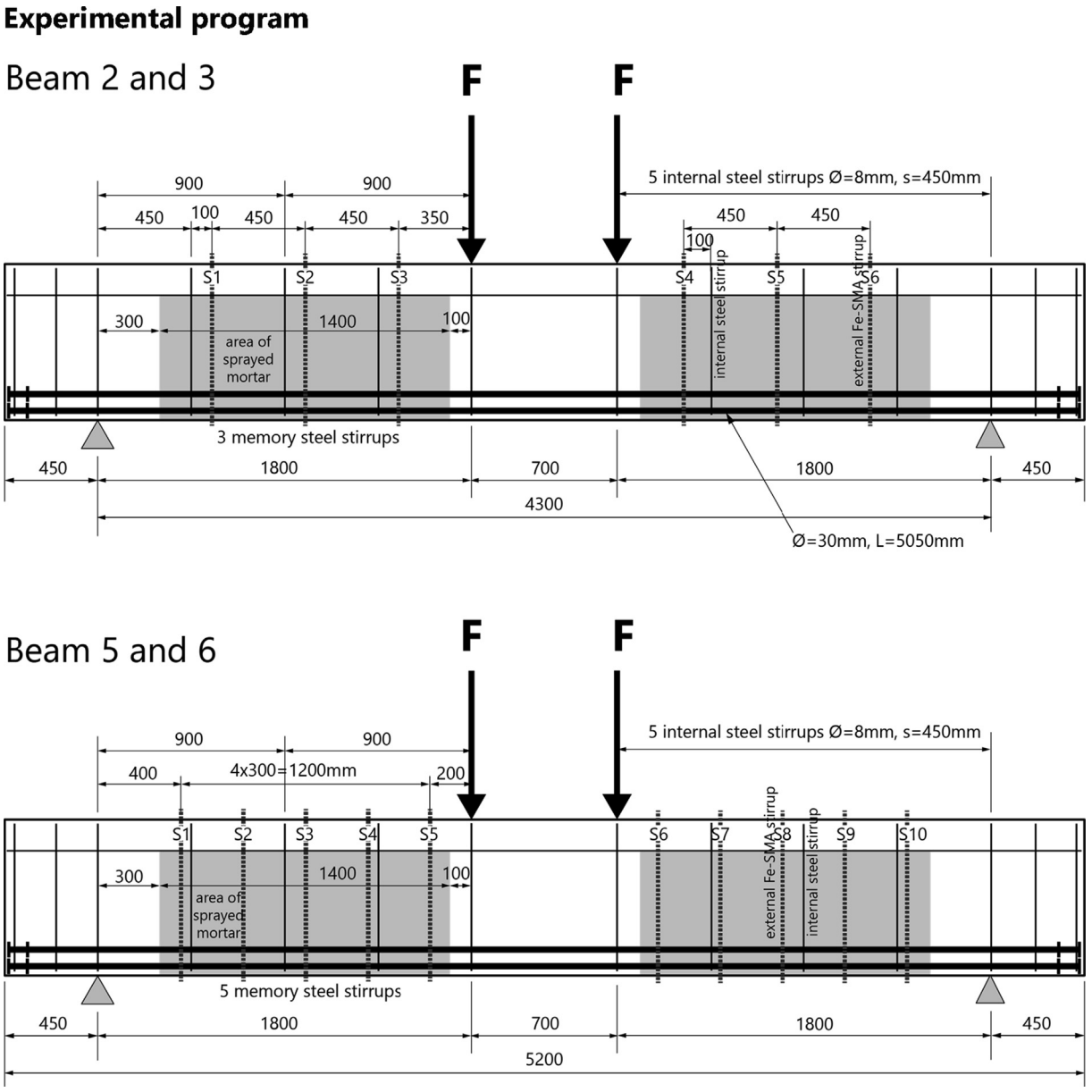

Fig. 7. Geometry and reinforcement of the beams.

Table 1
Overview of the experimental program. Concrete strength of the test beams at the day of failure tests ($f_{cm,cube}$: compression test on three cubes 150 mm^3, f_{ctm}: splitting tensile test on three cubes 150 mm^3).

	Internal steel stirrups in a shear span	External memory-steel stirrups in a shear span	memory-steel prestressed	$f_{c,cube}$ MPa	f_{ct} MPa
Beam 1	3	–	–	48.1	3.90
Beam 2	3	3	Yes	46.5	3.45
Beam 3	3	3	No	43.5	3.45
Beam 4 (the repaired Beam 1)	damaged	3	Yes	–	–
Beam 5	3	5	Yes	58.7	4.85
Beam 6	3	5	No	42.1	3.25

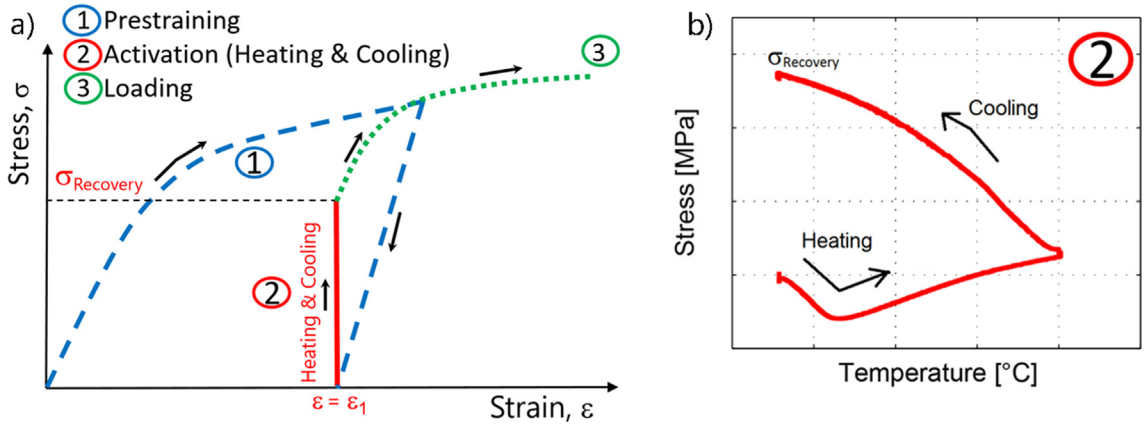

Fig. 8. a) Schematic of three main actions of application of memory-steel to strengthen and prestress a RC structure. b) Schematic illustration of the activation, Action (2), and the recovery stress development.

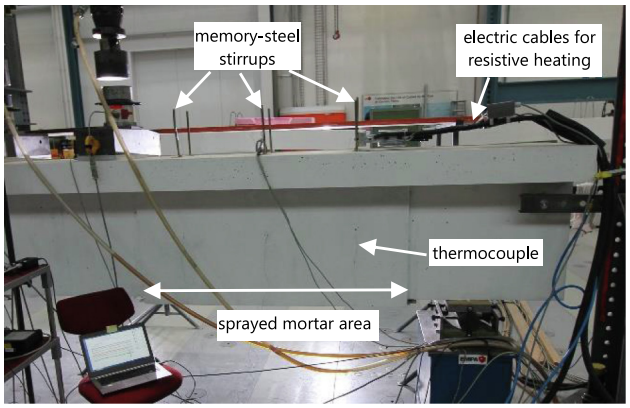

Fig. 9. One side of Beam 2 with the sprayed mortar area, the thermocouples for the temperature measurements during activation, and the U-shaped memory-steel stirrups which are visible on the top side.

Fig. 10. Detail of the cooper clamps for the connection of the electric power supply (resistive heating) with the U-shaped memory-steel stirrups on Beam 2.

tures given in Fig. 11. The temperatures were measured with thermocouples (Fig. 9), which were attached to the stirrups before the casting. It is visible in Fig. 11, that the maximum temperatures were reached after 1.5 min, whereas the cooling down to room temperature needed approximately 20 min. For the ribbed memory-steel bars, a prestress of approximately 300 MPa can be expected for heating temperatures measured in Fig. 11. Therefore, if a web width of 220 mm is assumed (including the sprayed mortar), Beam 2 and 5 with three and five memory-steel stirrups had before the start of the loading experiment vertical compression stress in the concrete web of approximately 0.6 MPa and 0.9 MPa, respectively.

Lastly, **Action (3)**, when the concrete structure was loaded, the memory-steel U-shaped stirrups performed as shown in Fig. 8a.

2.5. Experimental set-up

The beams were investigated in a four-point bending loading scheme (Fig. 7 and Fig. 12). The loading was applied by using two 1000 kN hydraulic jacks. The beams were supported by two rolling supports, one of them horizontally fixed.

2.6. Measurements

Beside conventional mid-span displacement with LVDT's, strain gauge measurements (designation SG in Fig. 13) and load cells, also digital image correlation (DIC) measurements were performed (Fig. 12) with two measurement fields (gray area in Fig. 13) on both shear spans to monitor the crack pattern and crack width developments. Strain gauges were not attached to the memory-steel stirrups, because the memory-steel stirrups were heated to 160–200 °C, what could damage the strain gauges.

2.7. Repair of a damaged beam

As described in the overview of the experimental program in Table 1, besides the investigation of new beams, also a beam, which was loaded to failure was repaired and then tested again. To be more specific, the reference beam without strengthening (Beam 1) was repaired after the failure test. Firstly, the large shear cracks in Beam 1 were closed at the sides with a mortar (Sika FastFix-121) and subsequently injected with a two-part injection grout (Sika InjectoCem-190), Fig. 14. Afterward, the same strengthening steps as described above (Steps 1 to 9) were performed (Fig. 15). Then, the beam was loaded to failure. The experiment on the repaired beam was designated as Beam 4. The internal steel stirrups, which ruptured during the failure test on Beam 1 were not

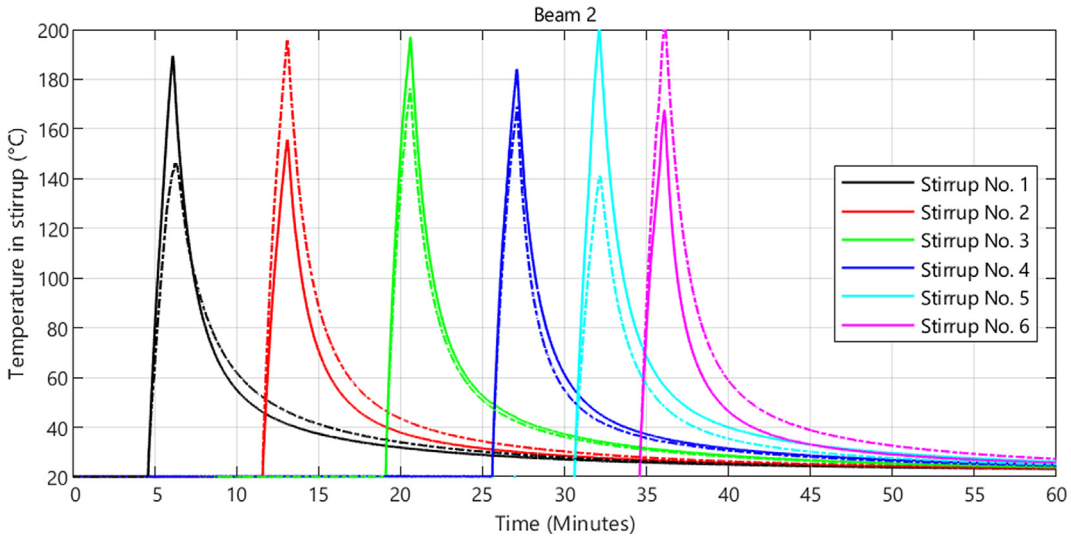

Fig. 11. Measured temperatures of the memory-steel stirrups in Beam 2 during their activation. The numbering of the stirrups is given in Fig. 7. For each stirrup, two measurements were executed.

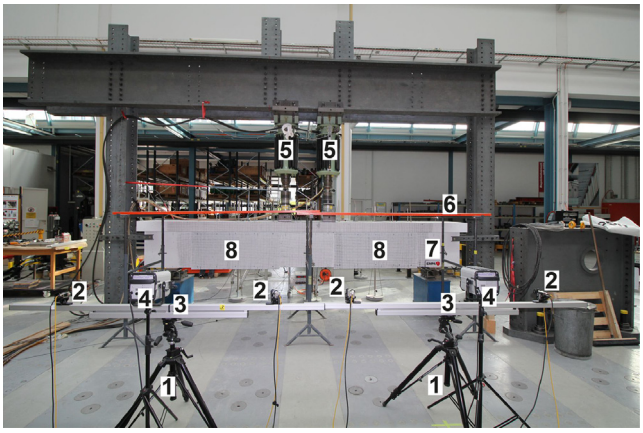

Fig. 12. Set-up for the large-scale experiments (1: tripods and 2: cameras for the both DIC systems, 3: beam supports, 4: lamps for DIC measurements, 5: oil hydraulic loading cylinders, 6: wooden plates for light shielding for DIC measurements, 7: test beam, 8: area of sprayed mortar).

repaired. The results of the Beam 1 and 4 were presented already in [33].

3. Results

3.1. Failure modes

All beams failed in shear (Fig. 16). In all beams, the internal stirrups yielded and ruptured before the shear failure of the beams. Rupture of the internal steel stirrups was hearable and some were visible via the large cracks (Fig. 17). Yielding of the stirrups resulted in the formation of shear cracks with large widths (Fig. 16). However, the memory-steel stirrups did not rupture (Fig. 17). At shear failure, the Beams 2 to 6 showed a compression failure of the flange under the loading point (Fig. 16b and c), which was not observed in the reference test beam (Beam 1), see Fig. 16a.

Additional to the shear cracking behavior in the web, visible in Fig. 16, cracks in the flange on the top side of the beams could be observed. Fig. 18 displays a photo of the cracks on the left (side of shear failure) top side of Beam 5 after the shear failure. The transverse cracks (No. 1 in Fig. 18) in cross-direction of the beam are bending cracks in the longitudinal direction, originating from the small shear stiffness in the longitudinal direction. However, the longitudinal cracks (No. 2 in Fig. 18 and Fig. 19) indicate a bending in cross-direction, which might originate from the shear failure of the beam. Furthermore, in some cases, a slight slip of the stirrups (Fig. 20) on the top side of the flange was observed after the failure tests, what might also originate from the shear failure of the beam.

3.2. Force-mid-span displacement

The force-mid-span displacement behaviors of all five beams are given in Fig. 21. The strengthening with the memory-steel stirrups and shotcrete mortar (increase of the web width from 160 to 220 mm) increased the failure forces by 86% (Table 2). Additionally, the mid-span displacements at a serviceability force of 200 kN are also compared in Table 2 and Fig. 21b. Shear strengthening decreased the mid-span considerably down to a minimum of 61% for the case of Beam 5.

By comparing the non-prestressed and prestressed memory-steel strengthening in Table 2 and Fig. 21, the following conclusions can be derived: (1) the failure force was not influenced by a prestress of the U-shaped memory-steel stirrups, however, (2) the beam displacements at serviceability was influenced by a prestress. In the case of three and five stirrups, the mid-span displacements were reduced if the stirrups were prestressed from 5.5 mm to 4.8 mm and from 4.8 mm to 4.4 mm (approximately 10% reduction), respectively. Smaller displacement is due to the higher shear stiffness of the cross-section if the stirrups are prestressed.

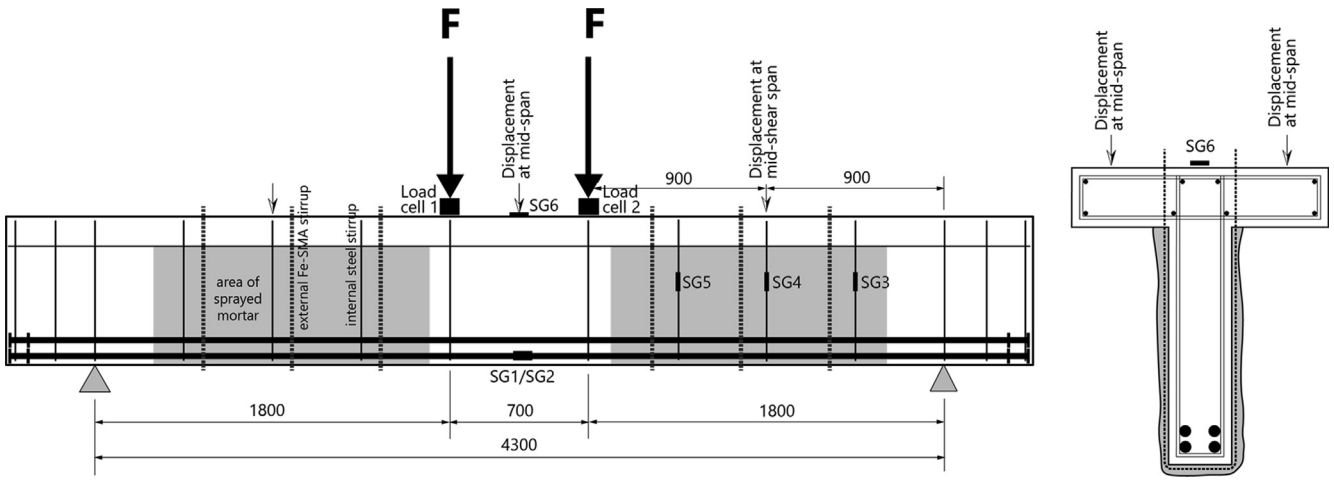

Fig. 13. Overview of the measurements performed during the loading experiments up to failure. Displacements, designation SG displays the strain gauge measurements on the internal steel reinforcements and on the concrete surface, load cells for the load, the gray area designates the fields of the DIC measurements.

Fig. 14. Beam 1 after failure tests. Injected shear cracks. The repaired beam was designated as Beam 4.

Fig. 15. Beam 4 after injection of shear cracks, concrete hammering, sandblasting, drilling of the holes in the flange, installation of the U-shaped ribbed memory-steel stirrups. The strengthening steps 5 to 9 are still missing in the photo.

Similar results were reported in [30], in which also beam failure tests with activated and non-activated memory-steel shear strengthening were presented. The failure loads of the beams with activated and non-activated memory-steel shear strengthening were similar, however, the appearance of shear cracks in the beams with activated shear strengthening were delayed.

The force-mid-span displacement behavior of the beam, which was loaded to failure two times is given in Fig. 22. As described before, firstly, it was tested as the reference unstrengthened beam (Beam 1), and secondly, it was loaded to failure after it was repaired and strengthened (Beam 4). It is visible, that the initial stiffness of Beam 4 is slightly lower as this is due to the flexural stiffness and the flexural cracks were already produced during the first loading. However, afterward, the shear stiffness is considerably higher what indicates that the shear strengthening is effective and works well. The failure mode of Beam 4 was the same as the Beams 2 to 6, namely a compression failure of the flange under the loading point Fig. 23). The failure load was even higher as Beam 1 which also shows that the repair and strengthening were successful.

3.3. Force-strain in flexural reinforcement and concrete at mid-span

The curves of the force-tensile strain in the flexural reinforcement and the force-compressive strain in the concrete, both at beam mid-span (Fig. 13), are given in Fig. 24. It is visible, that the tensile reinforcement stayed in elastic state and the concrete was clearly below 3000 μm/m, at which concrete crushing is usually expected. These measurements confirm that the design of the test beams was correct, predicting that shear failure occurs prior to bending failure.

3.4. Force-strain in internal steel stirrups

As displayed in Fig. 13, three strain gauges were applied to the internal steel stirrups. However, some of them were damaged during the strengthening work so that for Beam 2 only one and for Beam 6 only two strain measurement results were available. The

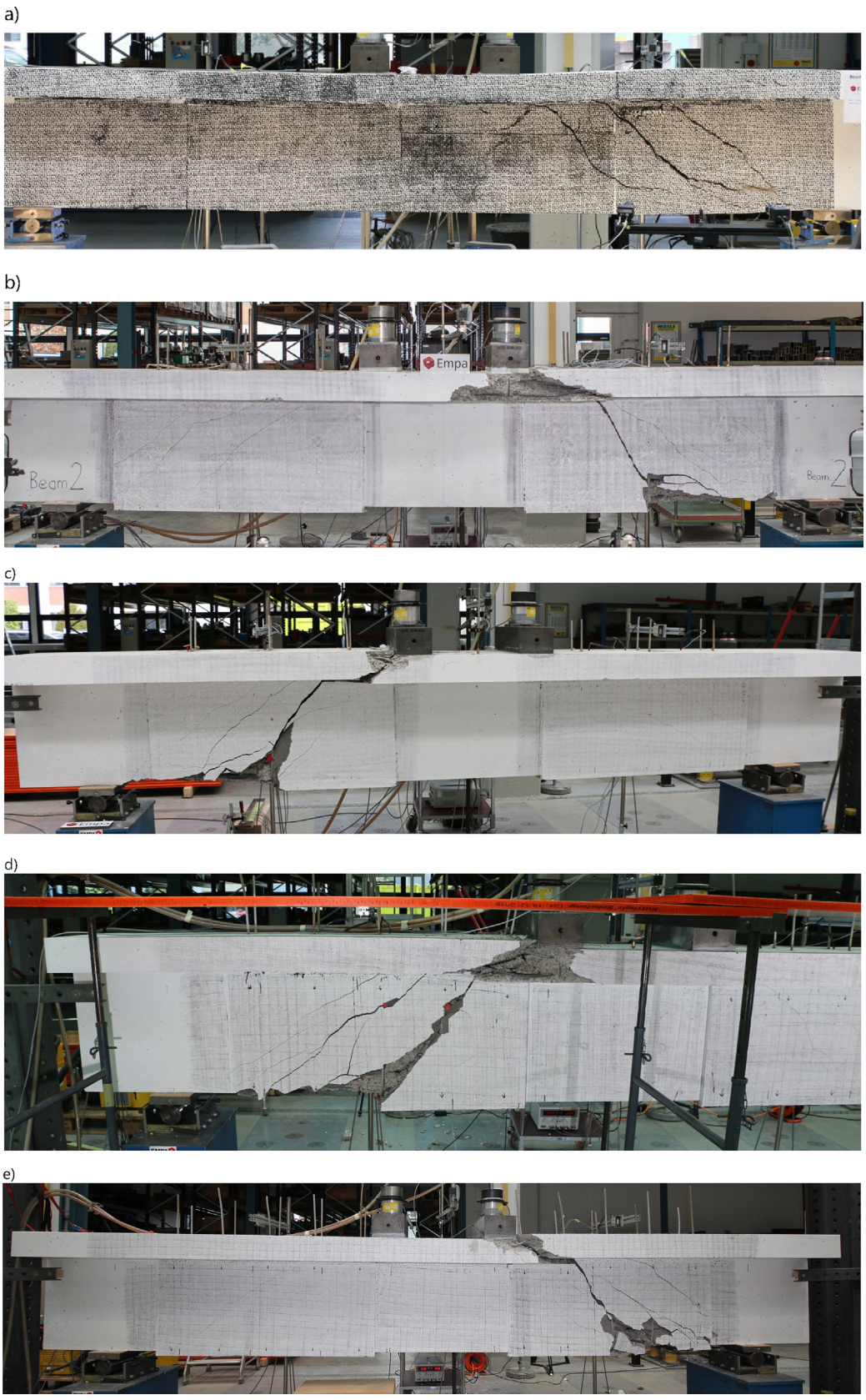

Fig. 16. Failure modes of a) Beam 1 (reference beam), b) Beam 2, c) Beam 3, d) Beam 5 and e) Beam 6.

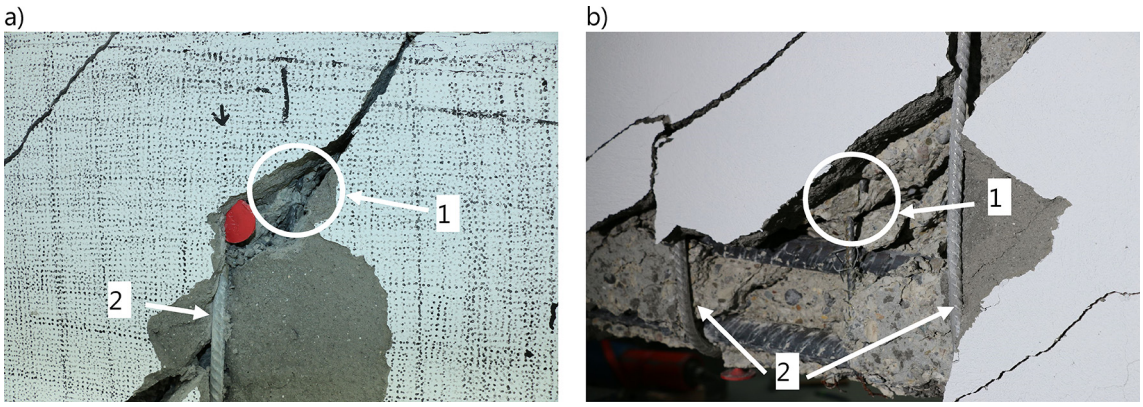

Fig. 17. Tensile failures of the internal steel stirrups after the failure test: a) in Beam 5, b) in Beam 6 (1: internal steel stirrups, 2: external applied memory-steel stirrups in sprayed mortar layer).

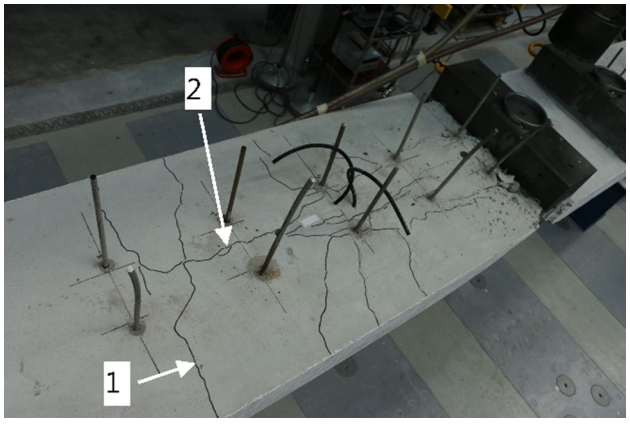

Fig. 18. Beam 5: 1) transverse cracks and 2) longitudinal cracks on the left beam top side (side of shear failure).

Fig. 19. Beam 5: only one longitudinal crack on the right beam top side (the side with no shear failure).

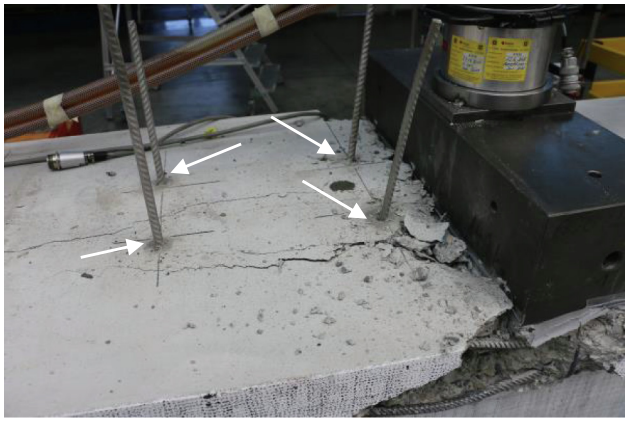

Fig. 20. Beam 5: arrows are indicating the slip of the memory-steel stirrups after the shear failure.

measured strains in the internal steel stirrups are presented in Fig. 25. Firstly, the beneficial effect of the shear strengthening is visible, because the strains in the internal stirrups are lower in the strengthened beams compared to the reference beam. Secondly, the prestressing of the memory-steel stirrups reduced the strain in the internal steel stirrups even more, which can also be observed in Fig. 25a for the Beams 2 and 3 and Fig. 25b for the Beams 5 and 6.

3.5. Crack pattern and crack widths

As mentioned before, on both shear spans, the crack pattern and crack width developments were monitored by using a DIC system. The crack pattern development of Beam 2 and 3 is displayed in Fig. 26 for various load steps at the serviceability state in the force range of 50 to 150 kN. The influence of the prestressing of the memory-steel stirrups is mainly visible from the different inclinations of the cracks. The cracks in Beam 3 (non-prestressed) on the left side of the figure show more inclined cracks.

As Fig. 26 only shows the qualitative crack pattern development, the software ACDM was used to evaluate the continuous

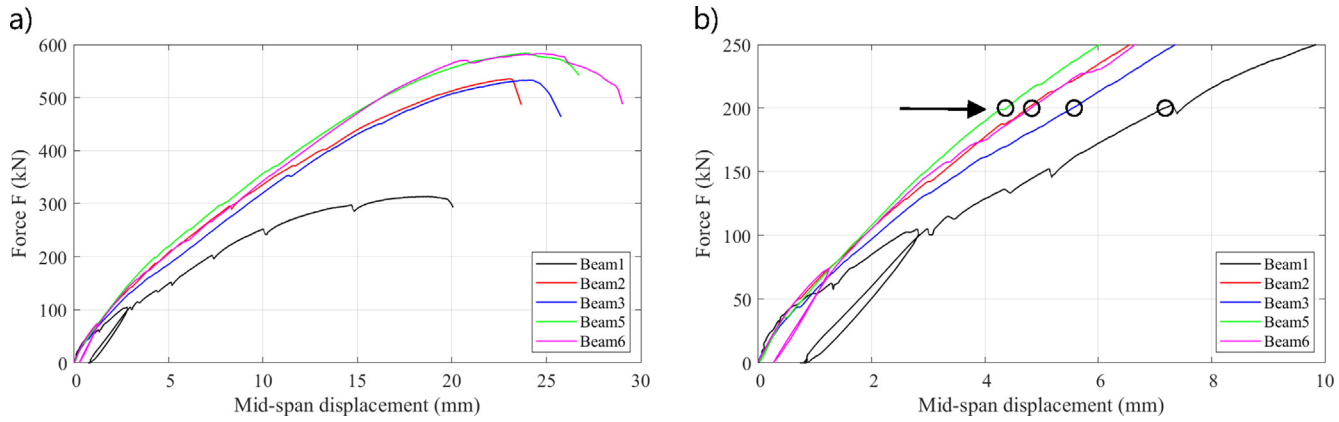

Fig. 21. a) Force-displacement diagrams of Beams 1 to 6 (without 4), b) zoom of a).

Table 2
Results of the large-scale experiments.

	Strengthening configuration	Maximum load F [kN]		Mid-span displacement [mm] at F = 200 kN	
Beam 1		313.4	100%	7.2	100%
Beam 2	3 stirrups prestressed	535.5	171%	4.8	66%
Beam 3	3 stirrups	532.7	170%	5.5	77%
Beam 4 (the repaired Beam 1)	damaged	409.1	131%	5.4	75%
Beam 5	5 stirrups prestressed	583.6	186%	4.4	61%
Beam 6	5 stirrups	583.0	186%	4.8	67%

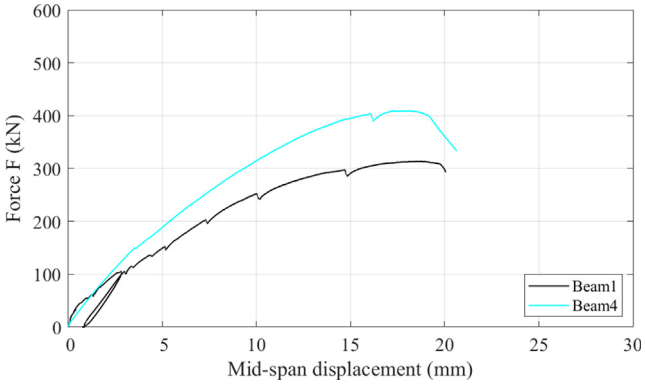

Fig. 22. Force-displacement diagram of Beams 1 and 4.

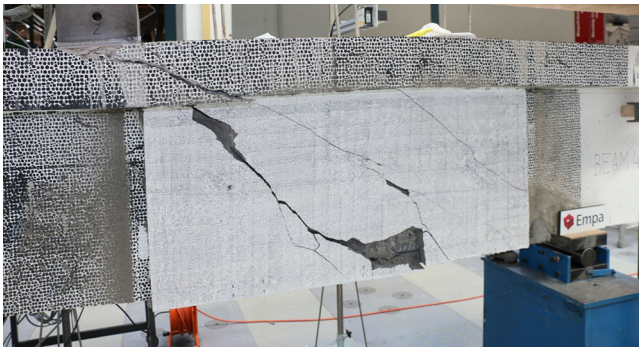

Fig. 23. Failure mode of Beam 4.

crack widths. The software was developed at the Institute of Structural Engineering at the ETH Zürich in Switzerland [34]. In Fig. 27 and Fig. 28, the continuous crack widths at the load stage 150 kN of Beam 2, Beam 3, and Beam 5, Beam 6 are given, respectively. Additionally, in the figures, the mean values of all cracks, the mean absolute value of the crack slips, and the number of cracks are presented.

The influence of prestressing on the crack widths is visible in Fig. 27; crack widths are smaller and the cracks are less inclined in Beam 2, which had prestressed memory-steel stirrups. Also, the number of cracks is smaller. The same can be observed in Fig. 28 with Beam 5, which was prestressed. For example, it is visible in Fig. 27, that Beam 2 with prestressed memory-steel stirrups had on the left shear span a mean crack width of 0.059 mm, whereas Beam 3 with non-prestressed memory-steel stirrups had a mean crack width of 0.092 mm, what is more than 50% larger.

With Fig. 27 and Fig. 28, the influence of using three or five stirrups can be observed. The beams with five stirrups had less inclined cracks than the beams with three stirrups, however, the crack widths were similar.

3.6. Design

From this research work, it can be concluded, that the ultimate limit state of shear design can performed by neglecting the prestressing force in the shear reinforcement and using the usual equations as given in the codes and guidelines. However, the serviceability limit state of shear design is strongly influenced by the prestressing force in the shear reinforcement. More work is necessary to work out a design concept to consider this effect.

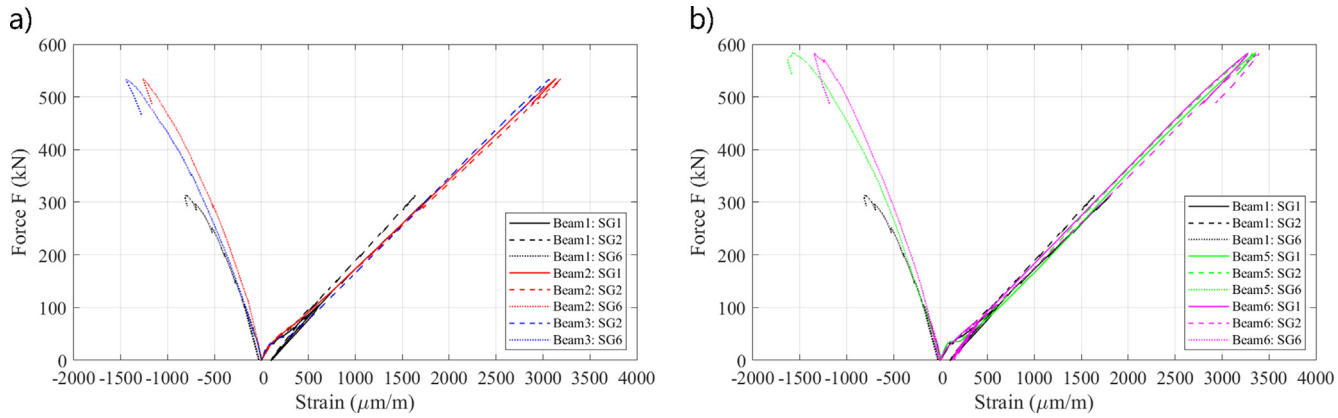

Fig. 24. Force-tensile strain in flexural reinforcement and compressive strain in the concrete of Beam 1 compared with a) Beam 2 and 3 (three stirrups) and b) Beam 5 and 6 (five stirrups) at beam mid-span (Fig. 13).

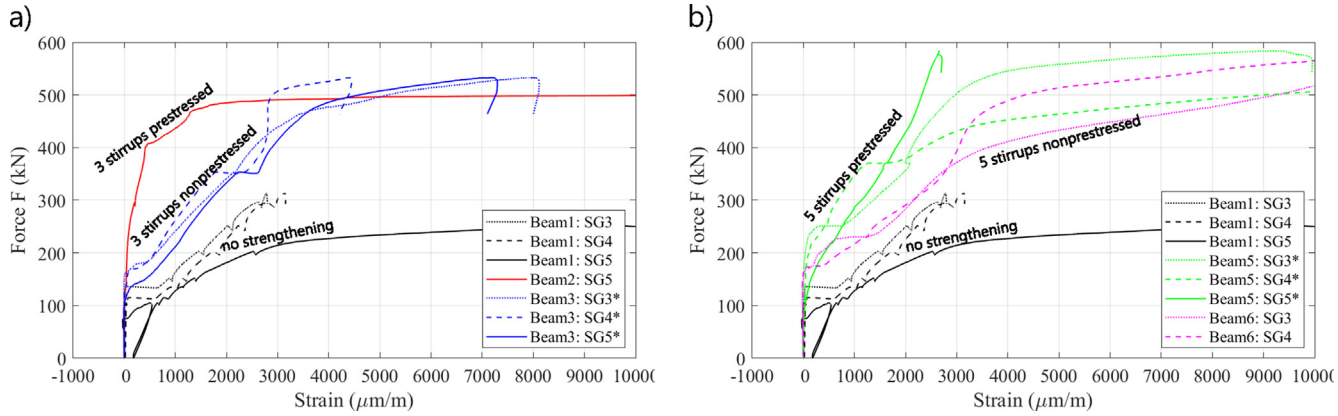

Fig. 25. Force-tensile strain in internal steel stirrups (shear reinforcement) in Beam 1 compared with a) Beam 2 and 3 (three stirrups) and b) Beam 5 and 6 (five stirrups). (*: the location of the internal stirrups with strain gauges were not on the beam side with the shear failure).

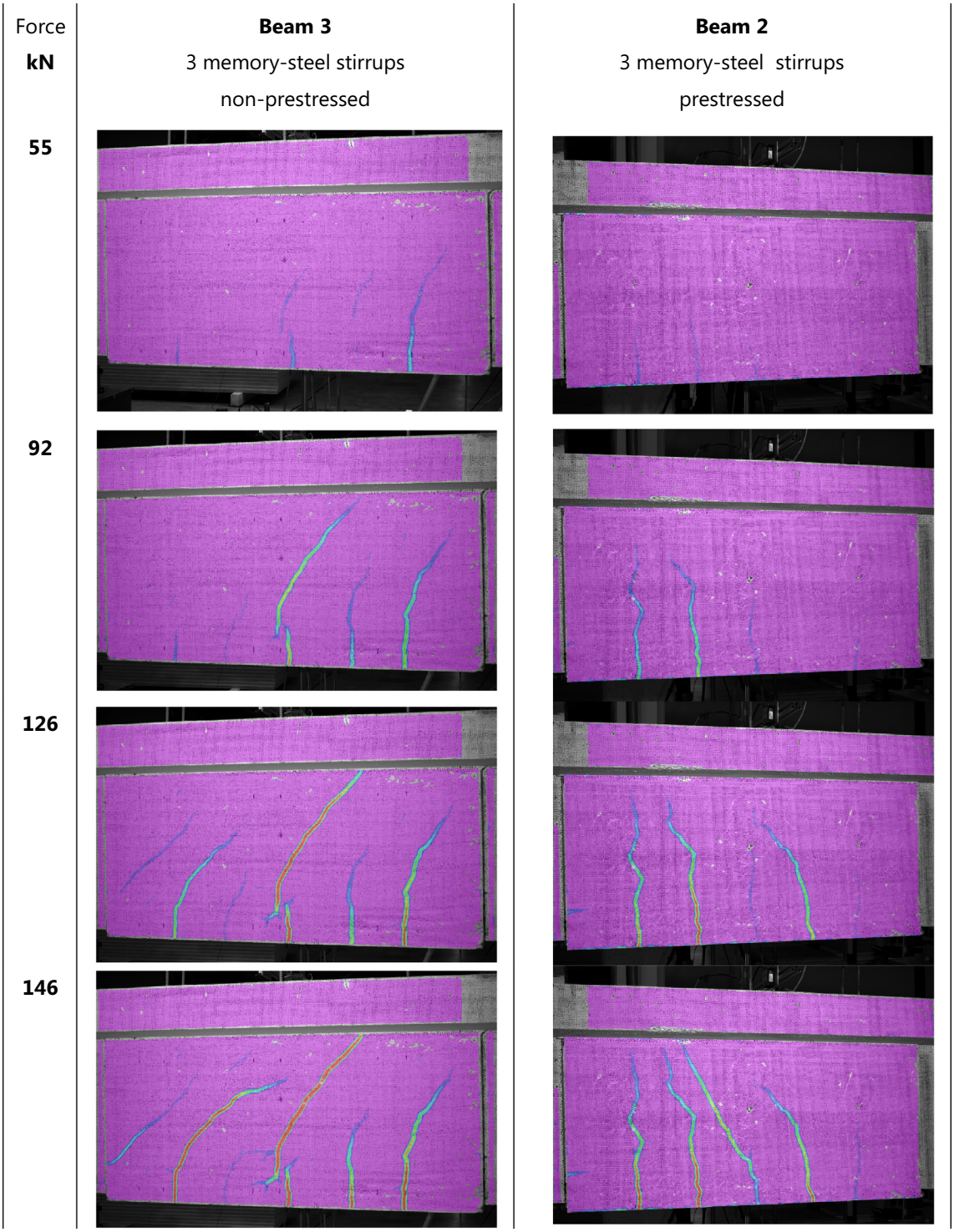

Fig. 26. Results of the DIC measurements, which were performed on the concrete surfaces on the beams 2 and 3 during the failure experiments as shown in Fig. 13. The figures display the maximum principal strains.

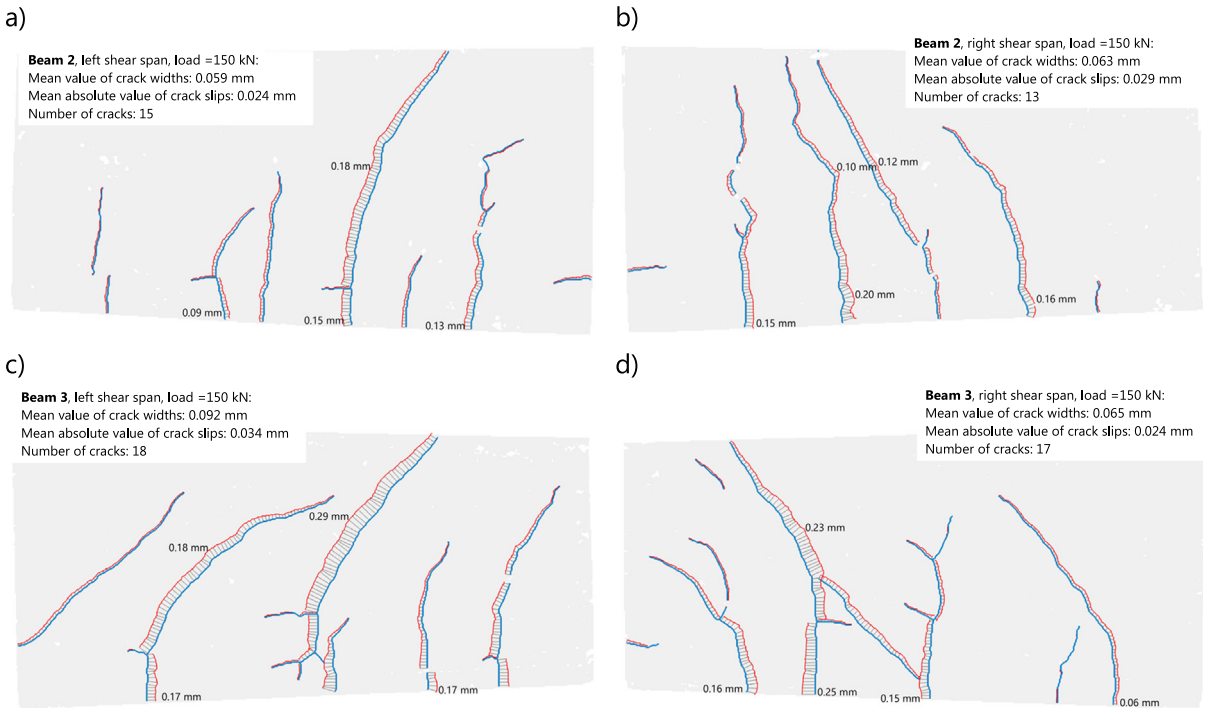

Fig. 27. Crack patterns and widths of the beams at a load of 150 kN: a) and b) Beam 2 (three prestressed stirrups), c) and d) Beam 3 (three non-prestressed stirrups).

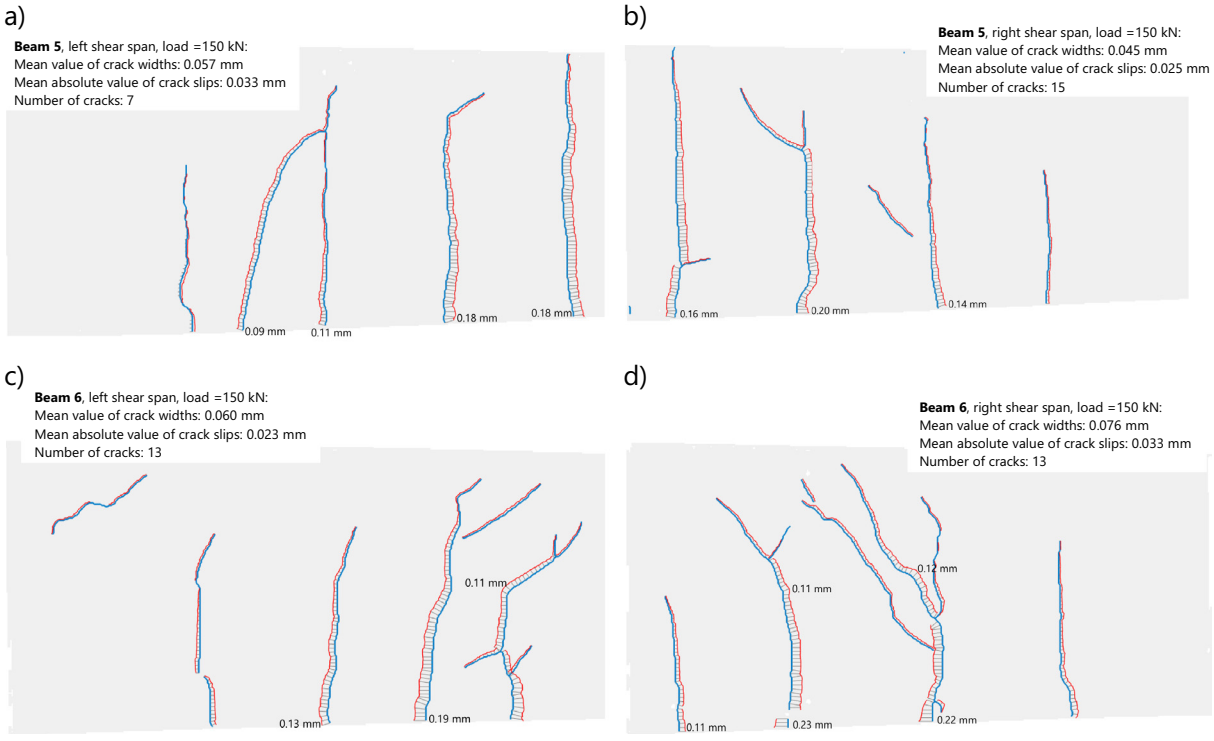

Fig. 28. Crack patterns and widths of the beams at a load of 150 kN: a) and b) Beam 5 (five prestressed stirrups), c) and d) Beam 6 (five non-prestressed stirrups).

4. Conclusion

This study on iron-based shape memory alloys for shear strengthening of concrete girders has revealed several aspects summarized as follows:

- The presented technique on U-shaped ribbed bars embedded in the shotcrete or sprayed mortar layer is a technically feasible method for on-site application without any major difficult tasks. All the performed steps starting with preparing the memory-steel stirrups over the surface preparation of the girders to finally embedding and activating the shape memory effect were demonstrated.
- The strengthening efficiency could be demonstrated by several static large-scale experiments. By adding additional stirrups, load-bearing capacity could be substantially increased. The failure occurred in shear by rupture of the internal steel stirrups and a subsequent crushing in the upper compression zone. No interface failure between the existing (and subsequently roughened) concrete surface and the new sprayed mortar layer was observed. The memory-steel stirrups did not rupture.
- Prestressing the memory-steel stirrups allowed to increase the load at which shear cracks appear. Furthermore, at identical load level, the width of shear cracks and beam mid-span displacements is smaller in case of prestressing than if initially unstressed memory-steel stirrups are used.
- Prestressing the memory-steel stirrups further reduced the stress level in the internal steel stirrups. This is particularly beneficial for applications in infrastructure constructions under cyclic loading and related fatigue problems.
- Lastly, the investigation showed also that it was possible to repair a heavily damaged beam by using the strengthening method presented in the paper.

CRediT authorship contribution statement

Christoph Czaderski: Conceptualization, Methodology, Investigation, Validation, Writing - original draft, Supervision, Funding acquisition, Project administration. **Moslem Shahverdi:** Conceptualization, Methodology, Investigation, Writing - review & editing, Validation. **Julien Michels:** Conceptualization, Methodology, Investigation, Resources, Writing - review & editing, Validation.

Declaration of Competing Interest

The authors declare that they have no known competing financial interests or personal relationships that could have appeared to influence the work reported in this paper.

Acknowledgements

The authors would like to express their thankfulness to the Commission for Technology and Innovation of Switzerland, which supported this research financially (CTI Project No. 18528.1 PFIW-IW). Further thanks go to the industry partner re-fer from Seewen in Switzerland, who delivered all the memory-steel and also supported this research financially. Lastly, the financial and technical support of the Empa Structural Engineering Research Laboratory is greatly appreciated.

References

[1] ASCE. https://www.infrastructurereportcard.org/cat-item/bridges/. 2017.
[2] SIA166, Klebebewehrungen (Externally bonded reinforcement), 2004, Zurich, Switzerland: Schweizerischer Ingenieur- und Architektenverein, SIA. pages 44.
[3] Masoud Motavalli, Christoph Czaderski, Kerstin Pfyl-Lang, Prestressed CFRP for strengthening of reinforced concrete structures: recent developments at Empa, Switzerland, J. Compos. Constr. 15 (2) (2011) 194–205.
[4] Christoph Czaderski, Masoud Motavalli, Fatigue behaviour of CFRP L-shaped plates for shear strengthening of RC T-beams, Compos. B Eng. 35 (4) (2004) 279–290.
[5] J.M. Lees, A.U. Winistörfer, U. Meier, External prestressed carbon fiber-reinforced polymer straps for shear enhancement of concrete, J. Compos. Constr. 6 (4) (2002) 249–256.
[6] Robert M. Foster, Monika Brindley, Janet M. Lees, Tim J. Ibell, Chris T. Morley, Antony P. Darby, Mark C. Evernden, Experimental investigation of reinforced concrete T-beams strengthened in shear with externally bonded CFRP sheets, J. Compos. Constr. 21 (2) (2017) 04016086, https://doi.org/10.1061/(ASCE)CC.1943-5614.0000743.
[7] S.J.E. Dias, J.A.O. Barros, NSM shear strengthening technique with CFRP laminates applied in high T cross section RC beams, Compos. B Eng. 114 (2017) 256–267.
[8] Ahmed Godat, Farah Hammad, Omar Chaallal, State-of-the-art review of anchored FRP shear-strengthened RC beams: a study of influencing factors, Compos. Struct. 254 (2020) 112767, https://doi.org/10.1016/j.compstruct.2020.112767.
[9] E. Moradi, H. Naderpour, A. Kheyroddin, An experimental approach for shear strengthening of RC beams using a proposed technique by embedded through-section FRP sheets, Compos. Struct. 238 (2020) 111988, https://doi.org/10.1016/j.compstruct.2020.111988.
[10] A. Winistörfer, Development of non-laminated advanced composites straps for civil engineering applications (Ph.D. thesis), 1999, University of Warwick, U.K. p. 170.
[11] J.M. Lees, A.U. Winistörfer, Nonlaminated FRP strap elements for reinforced concrete, timber, and masonry applications, J. Compos. Constr. 15 (2) (2011) 146–155.
[12] Feifei Jin, Janet M. Lees, Experimental behavior of CFRP strap–strengthened RC beams subjected to sustained loads, J. Compos. Constr. 23 (3) (2019) 04019012, https://doi.org/10.1061/(ASCE)CC.1943-5614.0000936.
[13] Julien Michels, Moslem Shahverdi, Christoph Czaderski, Flexural strengthening of structural concrete with iron-based shape memory alloy strips, Struct. Concr. 19 (3) (2018) 876–891.
[14] J. Michels, M. Shahverdi, C. Czaderski, R. El-Hacha, Mechanical performance of iron-based shape-memory alloy ribbed bars for concrete prestressing, ACI Mater. J. 115 (6) (2018) 877–886.
[15] L. Janke, C. Czaderski, M. Motavalli, J. Ruth, Applications of shape memory alloys in civil engineering structures – overview, limits and new ideas, Mater. Struct. 38 (279) (2005) 578–592.
[16] Moslem Shahverdi, Christoph Czaderski, Philipp Annen, Masoud Motavalli, Strengthening of RC beams by iron-based shape memory alloy bars embedded in a shotcrete layer, Eng. Struct. 117 (2016) 263–273.
[17] Elyas Ghafoori, Martin Neuenschwander, Moslem Shahverdi, Christoph Czaderski, Mario Fontana, Elevated temperature behavior of an iron-based shape memory alloy used for prestressed strengthening of civil structures, Constr. Build. Mater. 211 (2019) 437–452.
[18] Christoph Czaderski, Bernd Hahnebach, Masoud Motavalli, RC beam with variable stiffness and strength, Constr. Build. Mater. 20 (9) (2006) 824–833.
[19] A. Cladera, B. Weber, C. Leinenbach, C. Czaderski, M. Shahverdi, M. Motavalli, Iron-based shape memory alloys for civil engineering structures: an overview, Constr. Build. Mater. 63 (2014) 281–293.
[20] A. Sato, E. Chishima, K. Soma, T. Mori, Shape memory effect in $\gamma \rightleftarrows \varepsilon$ transformation in Fe-30Mn-1Si alloy single crystals, Acta Metall. 30 (6) (1982) 1177–1183.
[21] Zhizhong Dong, Ulrich E. Klotz, Christian Leinenbach, Andrea Bergamini, Christoph Czaderski, Masoud Motavalli, A novel Fe-Mn-Si shape memory alloy with improved shape recovery properties by VC precipitation, Adv. Eng. Mater. 11 (1-2) (2009) 40–44.
[22] https://www.re-fer.eu/.
[23] Moslem Shahverdi, Julien Michels, Christoph Czaderski, Masoud Motavalli, Iron-based shape memory alloy strips for strengthening RC members: material behavior and characterization, Constr. Build. Mater. 173 (2018) 586–599.
[24] Moslem Shahverdi, Christoph Czaderski, Masoud Motavalli, Iron-based shape memory alloys for prestressed near-surface mounted strengthening of reinforced concrete beams, Constr. Build. Mater. 112 (2016) 28–38.
[25] C. Czaderski, M. Shahverdi, R. Brönnimann, C. Leinenbach, M. Motavalli, Feasibility of iron-based shape memory alloy strips for prestressed strengthening of concrete structures, Constr. Build. Mater. 56 (2014) 94–105.
[26] Parviz Soroushian, Ken Ostowari, Ali Nossoni, Habibur Chowdhury, Repair and strengthening of concrete structures through application of corrective posttensioning forces with shape memory alloys, Transp. Res. Rec. 1770 (1) (2001) 20–26.
[27] Benito Mas, Antoni Cladera, Carlos Ribas, Experimental study on concrete beams reinforced with pseudoelastic Ni-Ti continuous rectangular spiral reinforcement failing in shear, Eng. Struct. 127 (2016) 759–768.
[28] Joan M. Rius, Antoni Cladera, Carlos Ribas, Benito Mas, Shear strengthening of reinforced concrete beams using shape memory alloys, Constr. Build. Mater. 200 (2019) 420–435.
[29] Luis A. Montoya-Coronado, Joaquín G. Ruiz-Pinilla, Carlos Ribas, Antoni Cladera, Experimental study on shear strengthening of shear critical RC beams using iron-based shape memory alloy strips, Eng. Struct. 200 (2019) 109680, https://doi.org/10.1016/j.engstruct.2019.109680.

[30] Antoni Cladera, Luis A. Montoya-Coronado, Joaquín G. Ruiz-Pinilla, Carlos Ribas, Shear strengthening of slender reinforced concrete T-shaped beams using iron-based shape memory alloy strips, Eng. Struct. 221 (2020) 111018, https://doi.org/10.1016/j.engstruct.2020.111018.
[31] L. Zerbe, M. Reda, M. Dawood, A. Belarbi, A. Senouci, B. Gencturk, M. Al-Ansari, J. Michels, Behavior of Retrofitted Concrete Members Using Iron-Based Shape Memory Alloys, in: SMAR 2017, Zurich, Switzerland, 13-15 September 2017, 2017.
[32] Carlos Rodrigo Ribas González, Miguel Fernández Ruiz, Influence of flanges on the shear-carrying capacity of reinforced concrete beams without web reinforcement: RIBAS GONZÁLEZ AND FERNÁNDEZ RUIZ, Struct Concrete 18 (5) (2017) 720–732.
[33] M. Shahverdi, C. Czaderski, J. Michels, 'memory steel' for Shear Reinforcement of Concrete Structures, SMAR 2019, 2019.
[34] Nicola Gehri, Jaime Mata-Falcón, Walter Kaufmann, Automated crack detection and measurement based on digital image correlation, Constr. Build. Mater. 256 (2020) 119383, https://doi.org/10.1016/j.conbuildmat.2020.119383.